Vol. 18, pp. 108–115 (2021)
doi: 10.2142/biophysico.bppb-v18.012

Biophysics and Physicobiology
https://www.jstage.jst.go.jp/browse/biophysico/

Regular Article

Role of Thr82 for the unique photochemistry of TAT rhodopsin

Teppei Sugimoto[1], Kota Katayama[1,2] and Hideki Kandori[1,2]

[1] *Department of Life Science and Applied Chemistry, Nagoya Institute of Technology, Nagoya, Aichi 466-8555, Japan*
[2] *OptoBioTechnology Research Center, Nagoya Institute of Technology, Nagoya, Aichi 466-8555, Japan*

Received March 12, 2021; accepted April 14, 2021; Released online in J-STAGE as advance publication April 16, 2021

Marine bacterial TAT rhodopsin possesses the pKa of the retinal Schiff base, the chromophore, at neutral pH, and photoexcitation of the visible protonated state forms the isomerized 13-*cis* state, but reverts to the original state within 10^{-5} sec. To understand the origin of these unique molecular properties of TAT rhodopsin, we mutated Thr82 into Asp, because many microbial rhodopsins contain Asp at the corresponding position as the Schiff base counterion. A pH titration study revealed that the pKa of the Schiff base increased considerably in T82D (>10.5), and that the pKa of the counterion, which is likely to be D82, is 8.1. It was thus concluded that T82 is the origin of the neutral pKa of the Schiff base in TAT rhodopsin. The photocycle of T82D TAT rhodopsin exhibited strong pH dependence. When pH is lower than the pKa of the counterion (pH <8.1), formation of the primary K intermediate was observed by low-temperature UV-visible spectroscopy, but flash photolysis failed to monitor photointermdiates at $>10^{-5}$ sec. The results were identical for the wild-type TAT rhodopsin. In contrast, when pH was higher than the pKa of the counterion, we observed the formation of the M intermediate, which decayed with the time constants of 3.75 ms and 12.2 sec. It is likely that the protonation state of D82 dramatically switches the photoreaction dynamics of T82D, whose duration lies between $<10^{-5}$ sec and >10 sec. It was thus concluded that T82 is one of the determinants of the unique photochemistry of TAT rhodopsin.

Key words: rhodopsin, retinal, photoisomerization, photocycle, protonation

Corresponding author: Hideki Kandori, Department of Life Science and Applied Chemistry, Nagoya Institute of Technology, Showa-ku, Nagoya, Aichi 466-8555, Japan. e-mail: kandori@nitech.ac.jp

Introduction

Rhodopsins are retinal-binding membrane proteins, which are classified into animal and microbial rhodopsins [1]. While animal rhodopsins are photosensory G-protein coupled receptors [1–4], microbial rhodopsins perform various functions, such as gene expression, enzymatic reactions and light-driven ion conductance such as pumps and channels [1,5–10]. Animal and microbial rhodopsins share a common seven transmembrane α-helical architecture with their N- and C-termini at the extracellular and intracellular sides, respectively, but they share almost no sequence homology. Microbial rhodopsins such as channelrhodopsins [11] are used as optogenetic tools [12,13]. The discovery of heliorhodopsins (HeRs) from microbes

◀ ***Significance*** ▶

Marine bacterial TAT rhodopsin possesses the pKa of the retinal Schiff base at neutral pH, and the primary photointermediate reverts to the original state within 10^{-5} sec. To identify the origin of these properties, here we investigated the T82D mutant. From a pH titration study, it was concluded that T82 is the origin of the neutral pKa of the Schiff base in TAT rhodopsin. The photocycle of T82D TAT rhodopsin was very slow (>10 sec) when D82 is negatively charged. It was thus concluded that T82 is one of the determinants of the unique photochemistry of TAT rhodopsin.

showed wide diversity of rhodopsins, as they have little sequential homology to known microbial rhodopsins and their membrane topology is opposite as to that of other rhodopsins [14].

All microbial rhodopsins feature all-*trans* retinal attached by a Schiff base linkage to the ε-amino group of a Lysine side chain in the middle of helix 7 [1,5–10]. Protonation of the all-*trans* retinal Schiff base is a common property of all microbial rhodopsins, providing a wide range of absorption and color tuning. To achieve high pKa of the positively charged Schiff base, microbial rhodopsins contain a counterion, which is composed of one or two negative charges [1,15]. Aspartate, glutamate and a chloride ion constitute the counterion, and protein-bound water molecules also play an important role. In the case of animal rhodopsins, UV-pigment contains an unprotonated Schiff base of 11-*cis* retinal in the resting stage [16–18]. Although microbial rhodopsins were previously believed to function using the protonated Schiff base in its ground state, some exceptions were recently reported. For example, a histidine kinase rhodopsin (HKR) from *Chlamydomonas reinhardtii* contains an unprotonated Schiff base when expressed in yeast cells [19,20]. Another example is TAT rhodopsin from a marine bacterium SAR11 HIMB114 [21,22]. TAT rhodopsin possesses a Schiff base with a pKa at neutral pH, suggesting the presence of both protonated and unprotonated forms at physiological pH. In addition to the atypical pKa of the Schiff base, light absorption of the protonated form of TAT rhodopsin causes retinal photoisomerization, but displays no formation of photointermediates at $>10^{-5}$ s [21].

What is the origin of the two unique properties, (i) low pKa of the Schiff base, and (ii) no photocycle completion, in TAT rhodopsin? Figure 1 compares the structure of a light-driven proton pump bacteriorhodopsin (BR) (a) and the structural model of TAT rhodopsin based on the BR structure (b). TAT rhodopsin was named because of the characteristic sequence motifs in the C helix [21], which correspond to the DTD (D85, T89 and D96) motif in BR. In BR, D85 and D212 in the G helix constitute the counterion complex, in which D85 is the primary counterion (Fig. 1a) [1]. In contrast, the TAT (T82, A86 and T93) motif indicates only one counterion at position 227 (Fig. 1b). Therefore, it is plausible that T82 contributes to lowering the Schiff base pKa in TAT rhodopsin. If so, does T82 contribute to the unusually fast photoreaction ($<10^{-5}$ sec)? In the present study, we prepared the T82D mutant of TAT rhodopsin, and compared its molecular properties with those of the wild-type (WT). Consequently, the pKa of the Schiff base increased considerably (>10.5), and the photocycle became >10 sec when D82 was deprotonated. The role of T82 in the unique molecular properties of TAT rhodopsin are discussed in the light of these results.

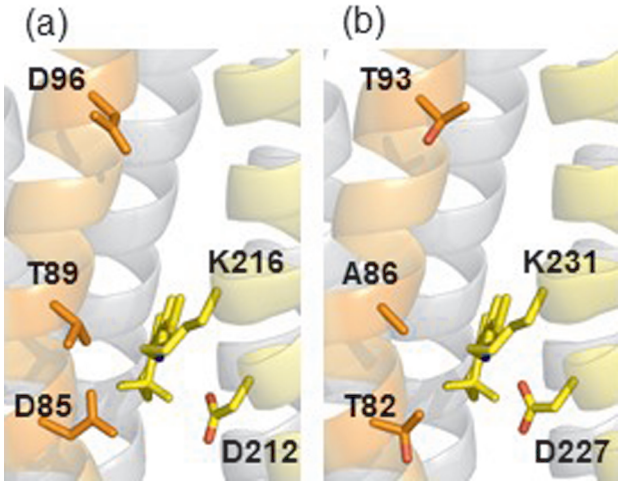

Figure 1 Structural comparison of (a) a light-driven proton-pump bacteriorhodopsin (BR), and (b) TAT rhodopsin. The structure of BR (PDB ID: 1C3W) was used for both models because of the lack of an atomic structure of TAT rhodopsin. In (b), residues of BR were replaced with those of TAT rhodopsin according to Supplementary Figure S1. The motif in the C-helix is DTD (D85, T89, D96) for BR (a), and TAT (T82, A86, T83) for TAT rhodopsin (b).

Materials and Methods

Protein expression and purification

The gene of SAR11 HIMB114 TAT rhodopsin, whose codon was optimized for an *Escherichia coli* expression system, was synthesized (Eurofins Genomics Inc.) and subcloned into a pET21a (+)-vector with a C-terminal 6×His-tag [21,22]. For mutagenesis, a Quick-change site-directed mutagenesis kit (Stratagene) was used based on a standard protocol [23,24]. WT and T82D mutant protein were expressed in the *E. coli* C43 (DE3) strain. The plasmid was prepared using the Nucleo Spin Plasmid Easy pure kit and 3 mL bacterial culture initiated from single colonies selected from a transformation plate. Protein expression was induced by 1.0 mM isopropyl β-D-thiogalactopyranoside (IPTG) for 4 h at 37°C in the presence of 10 μM all-*trans*-retinal (Sigma-Aldrich). The expressed proteins were purified from *E. coli* cells according to previously reported methods [23,24]. The cells were disrupted with a French Press (Ohtake) and the membrane fraction was collected by ultracentrifugation at 125,000 g for 1 h. The protein was solubilized in 2.0% *n*-dodecyl-β-D-maltoside (DDM) in the presence of 300 mM NaCl, 5 mM imidazole and 50 mM MES (pH 6.5). After Co^{2+}-NTA affinity chromatography, the collected fractions were dialyzed against a buffer containing 50 mM Tris–HCl pH 8.0, 150 mM NaCl and 0.03 % DDM to remove imidazole.

Measurement of absorption spectra and pH titration

To investigate the pH dependence of the absorption spectra of TAT rhodopsin, a solution containing 6 μM protein was solubilized in a six-mix buffer (10 mM citrate, 10 mM MES, 10 mM HEPES, 10 mM MOPS, 10 mM CHES and 10 mM CAPS) [21]. pH was changed by adding either concentrated HCl or NaOH. Absorption spectra were measured with a UV-visible spectrometer (V-2400PC, Shimadzu) at every ~0.5-pH change. The absorption maxima were plotted as a function of pH, and the data were fitted with the Henderson-Hasselbalch equation to determine the pKa of the counterion.

Laser flash photolysis

Time-evolution of the transient absorption changes of photo-excited WT and T82D TAT rhodopsins was observed as described previously [21,22]. The purified protein was resuspended in a buffer containing 50 mM Tris–HCl (pH 8.0), 150 mM NaCl and 0.03 % DDM. The sample solution was placed in a quartz cuvette and was excited with a beam of second harmonics of a nanosecond pulsed Nd^{3+}:YAG laser (λ=532 nm INDI40, Spectra-Physics). The excitation laser power was 3 mJ/pulse. The change in intensity of monochromated output of an Xe arc lamp (L9289-01, Hamamatsu Photonics, Japan) passed through the sample was observed by a photomultiplier tube (R10699, Hamamatsu Photonics) equipped with a notch filter (notch-wavelength=532 nm, NF03-532E-50×50, Semrock). The signal from the photomultiplier tube was averaged and stored in a digital-storage-oscilloscope (DPO7104, Tektronix, Japan). The obtained kinetics data were fitted by multi-exponential curves individually.

Low-temperature difference UV-visible spectroscopy

The WT and T82D TAT rhodopsins were reconstituted into a mixture of POPE and POPG (molar ratio=3:1) with a protein-to-lipid molar ratio of 1:50 by removing DDM with SM-2 BioBeads [21,22]. The pellet was resuspended in 1 mM NaCl and 2 mM MES (pH 6.0). Then, protein concentration was adjusted to 4.0 mg ml^{-1}. A 60 μl aliquot was placed onto a BaF_2 window and dried with an aspirator. Low-temperature UV-visible spectroscopy was applied to the films hydrated with H_2O at 77 K as described previously [21,22]. Samples were illuminated with 547±10 nm light (Toshiba) for 2 min for the formation of the K intermediate TAT rhodopsin. Reversion of the K intermediate to the resting state was attempted by illuminating the sample with >510-nm (O-53, AGC Techno Glass) light for 2 min.

Results

Molecular properties of the resting state in WT and T82D TAT rhodopsin

Figure 2 shows the absorption spectra of WT and T82D in detergent (0.03 % DDM) at pH 8.0. In the case of WT, two λ_{max} at 399 and 560 nm correspond to the deprotonated and protonated Schiff base, respectively (Fig. 2a). A previous pH titration study of WT reported the pKa as 7.3 in detergent (0.03 % DDM) and 8.4 in liposomes [21]. In contrast, the absorption spectrum of T82D possesses only one λ_{max} at 531 nm at pH 8.0 (0.03 % DDM) (Fig. 2b). This observation suggests that the newly introduced negative charge at position 82 increases the pKa of the Schiff base. The presence of a negative charge is supported by the λ_{max} at 531 nm, 29 nm blue-shifted from the WT (560 nm), as a negative charge near the Schiff base generally yields spectral blue shift in animal and microbial rhodopsins [1].

To further study the molecular properties of T82D TAT rhodopsin, we measured absorption spectra at different pHs. In the case of WT, the protonated form (560 nm) is dominant at pH 4 and the increase in pH induces the appearance of the unprotonated form (399 nm). The pH titration of WT can be described by the two states, which shows a clear isosbestic point at 451 nm [21]. Figure 3a shows the absorption spectra of T82D from pH 4 to pH 10.5, which are more complex than that of WT. At pH 4.0, the λ_{max} is located at 549 nm, which is blue-shifted when pH is increased. In addition, absorption at 380–400 nm

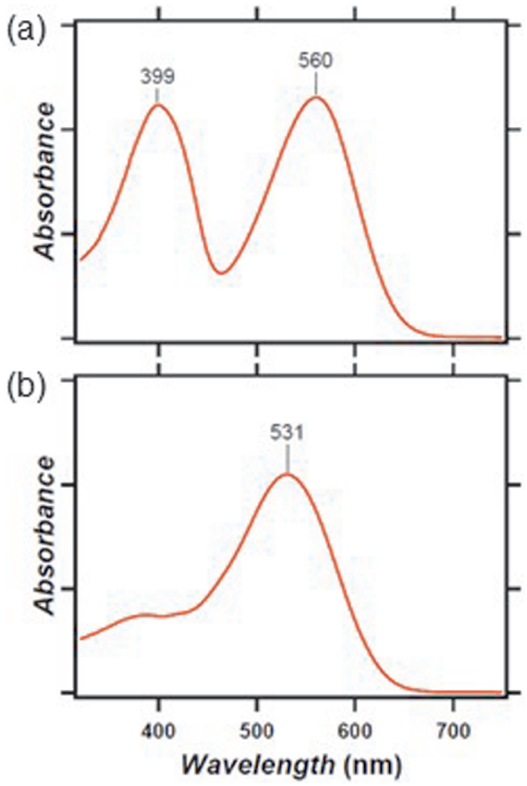

Figure 2 Absorption spectra of WT (a) and T82D (b) TAT rhodopsin, which were solubilized in 0.03 % DDM at pH 8.0. One division of the y-axis corresponds to 0.2 absorbance units.

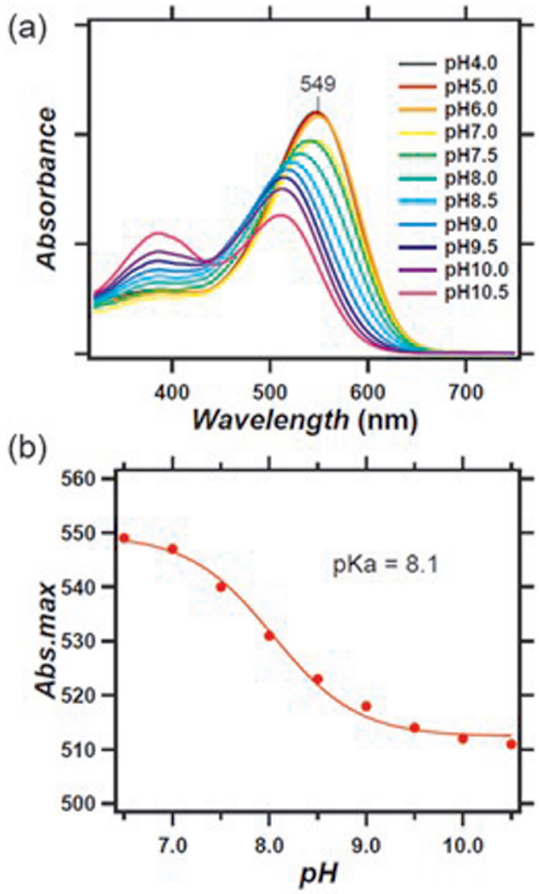

Figure 3 pH-dependent absorption changes of T82D TAT rhodopsin. (a) Absorption spectra of T82D TAT rhodopsin at pH 4 to 10.5. One division of the y-axis corresponds to 0.2 absorbance units. (b) pH-dependent changes of λ_{max}.

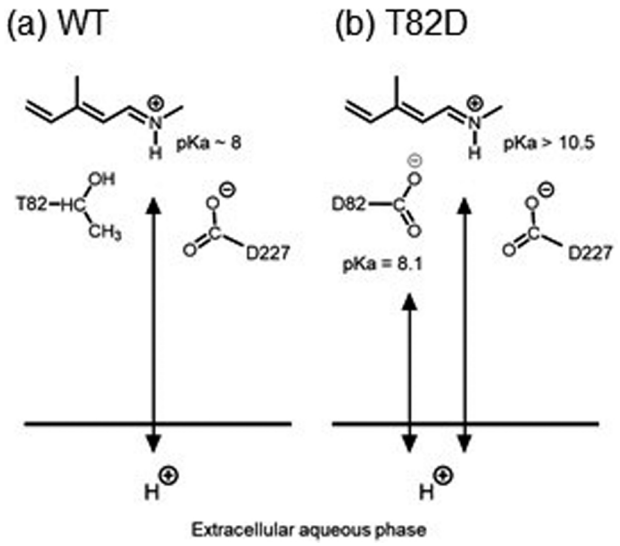

Figure 4 Structural model of WT (a) and T82D (b) TAT rhodopsin, where key residues are shown with the chromophore retinal on the extracellular side, which was revealed by recent electrophysiological measurements [22].

increases at pH >8. Thus, there are at least three states for T82D, unlike WT. The state of T82D, when absorbing at 380–400 nm, must have an unprotonated Schiff base. Although we attempted to determine the pKa, the equilibrium of the protonated and unprotonated Schiff base was only maintained up to pH 10.5, and higher pH led to an irreversible process due to aggregation. Thus, we were unable to determine the pKa value precisely, and concluded that the Schiff base pKa was higher than 10.5 in T82D TAT rhodopsin.

Figure 3b shows the pH titration of λ_{max} in the visible region, from which the pKa value was determined to be 8.1. This pKa is not owing to the Schiff base, as the λ_{max} is located at 510–550 nm. It is most likely owing to the pKa of the counterion of the Schiff base. Figure 4 illustrates the structural model of the Schiff base region of TAT rhodopsin. Recent electrophysiological measurements revealed that the extracellular pH affects the protonation equilibrium of the Schiff base [22]. In WT, D227 is the only counterion of the Schiff base, and the pKa of the Schiff base is 7.3 in detergent (0.1 % DDM) and 8.4 in liposomes (Fig. 4a) [21]. The pKa of the Schiff base significantly increases (pKa >10.5) by the T-to-D mutation at position 82 (Fig. 4b), indicating that T82 is the determinant of the unusually low pKa of the Schiff base in TAT rhodopsin.

In T82D, the origin of pKa at 8.1 is the counterion, and the straightforward interpretation of the origin is D82, as illustrated in Figure 4b. A previous phylogenetic analysis reported that TAT rhodopsin is homologous to bacterial light-driven proton-pumps such as proteorhodopsins (PRs), among which the closest protein in the amino-acid sequence is *Exiguobacterium sibiricum* rhodopsin (ESR) [21]. It is known that the pKa of the corresponding Asp is similarly high in ESR and PRs [25–27], which supports our interpretation of the origin of the pKa at 8.1 for D82. D227 is another candidate of the origin of the pKa (Fig. 1). While additional experiments are needed for conclusion, simple mutation study may not be sufficient as D82 and D227 constitute the counterion complex near the Schiff base. In ESR and PRs, the high pKa originates from the specific interaction between Asp and His in the B-helix [25–28]. The corresponding residue in TAT rhodopsin is Glu54 (Supplementary Fig. S1), which possibly interacts with D82 and raises the pKa.

Photoreaction dynamics of WT and T82D TAT rhodopsin

From the pH titration results of the T82D mutant, we can conclude that the low pKa of the Schiff base originates from T82. We next studied the photoreaction dynamics of T82D TAT rhodopsin in detergent after laser excitation at 532 nm. Since the counterion (D82) possesses a pKa at 8.1,

flash photolysis experiments should ideally be performed at pH 6 and pH 10, which contain the protonated and deprotonated counterion, respectively (Fig. 3a). However, the T82D protein was not stable at alkaline pH, easily forming aggregates. We thus applied flash photolysis to T82D at pH 6 and 8, the latter being a mixture of the protonated and deprotonated counterions.

Figure 5a shows the transient absorption result of T82D at pH 6, where absorbance was monitored near λ_{max} (550 nm). We did not observe any product formation, which was also the case for WT [21]. Previous low-temperature UV-visible and FTIR spectroscopy of WT TAT rhodopsin revealed that photoisomerization occurs from the all-*trans* to 13-*cis* form at 77 K, but the product returns to its original state without completing the photocycle [21]. When the counterion is protonated in T82D (pH 6), no product formation was observed at $>10^{-5}$ sec.

On the other hand, clear transient absorption was observed at pH 8 for T82D (Fig. 5b), whose photocycle was very long. Positive absorbance at 400 nm, together with the bleaching signal (520 nm), indicates the formation of the M intermediate, which appears with a time constant of 57 μsec, and half of the M intermediate decays with a time constant of 3.75 ms, while the other half decays with a time constant of 12.2 sec. We infer structural heterogeneity of the M intermediate, leading to either fast (3.75 ms) or slow (12.2 sec) decay to the resting state. The kinetic profile in Figure 5b suggests a comparable population of the

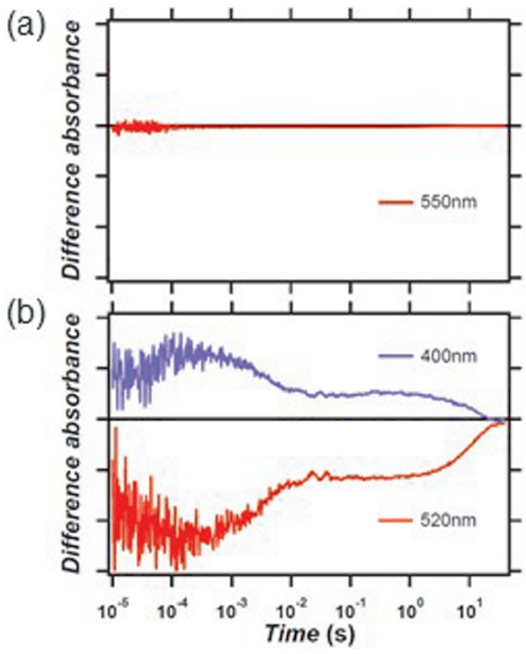

Figure 5 Photoreaction dynamics of T82D TAT rhodopsin at pH 6 (a) and pH 8 (b). Samples were excited at 532 nm, and transient absorption was monitored at 550 nm (a), and at 400 and 520 nm (b). One division of the y-axis corresponds to 0.004 absorbance units.

fast-decaying and slow-decaying M intermediates. However, other models are likely possible, so an additional and more comprehensive analysis of the photocycle, including numerous wavelengths and different pHs and other conditions, are needed. It should be noted that the photoreaction is unusually fast when D82 is protonated and neutral (pH 6), while the photocycle is prolonged more than seven orders of magnitude when D82 is deprotonated and negatively charged (pH 8). This indicates that T82 is the determinant of the unusually fast photoreaction of TAT rhodopsin.

Low-temperature UV-visible spectroscopy of WT and T82D TAT rhodopsin

Flash photolysis measurements failed to detect transient absorption at $>10^{-5}$ sec for T82D at pH 6 (Fig. 5a), which was also the case for WT [21]. In case of the protonated form of WT TAT rhodopsin, formation of the K intermediate was observed at 77 K, suggesting that primary photoisomerization takes place from the all-*trans* to 13-*cis* form as well as in other microbial rhodopsins, whereas the K intermediate returned to the original state without completing the photocycle [21]. In the present study, we applied low-temperature UV-visible spectroscopy to hydrated films of WT and T82D TAT rhodopsins under the same experimental conditions at 77 K. As shown in Figure 6, spectral red-shifts were observed for all samples. Note that the formation of the K intermediate was also the case for T82D at pH 6 (Fig. 6b), although transient absorption was not observed at $>10^{-5}$ sec (Fig. 5a).

In Figure 6, all difference spectra show broad negative bands at 400–550 nm, though λ_{max} of the unphotolyzed states are located at 560, 549 and 531 nm for WT, T82D at pH 6 and T82D at pH 8, respectively (Figs. 2 and 3a). On the other hand, positive peaks were relatively sharp, and their λ_{max} was located at 599, 582 and 562 nm for WT, T82D at pH 6 and T82D at pH 8, respectively. This tendency coincides with the λ_{max} at room temperature. The isosbestic points are located at 554, 541 and 533 nm, respectively. Thus, the molecular properties of T82D at pH 6 resemble those of WT. This is reasonable, as the residue at position 82 is neutral under these conditions (protonated Asp in T82D at pH 6 vs Thr in WT). In contrast, formation of the M intermediate was observed only at high pH, such as pH 8, suggesting that negatively charged D82 accepts a proton from the Schiff base in the M intermediate.

While normal formation of the K intermediate was observed for the three samples tested (Fig. 6), it should be noted that illumination of the K intermediate did not revert to the original state. This is unusual, as most primary intermediates of microbial and animal rhodopsins exhibit photochromism, such as the K and batho intermediates, respectively [29]. This was true not only for WT (Fig. 6a) and T82D at low pH (Fig. 6b), but also for T82D at high

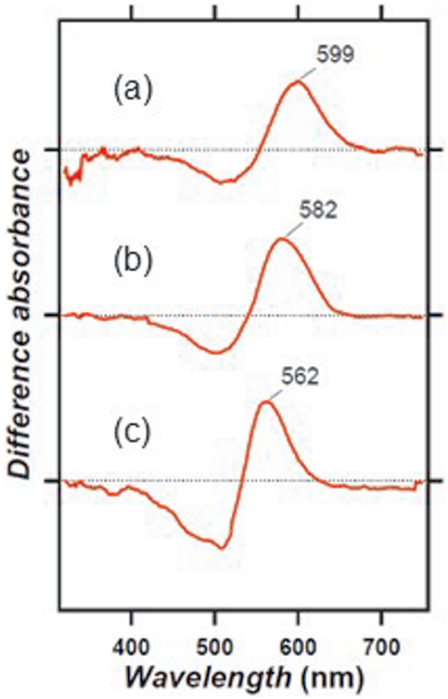

Figure 6 Light-induced difference UV-visible spectra of WT at pH 6 (a), T82D at pH 6 (b), and T82D at pH 8 (c). The sample was reconstituted into lipid membranes. Films hydrated with H_2O were illuminated at 547±10 nm, and the light-minus-dark difference spectra were measured. One division of the y-axis corresponds to 0.02 absorbance units.

pH (Fig. 6c), whose K intermediate was relaxed to the following M intermediate (Fig. 5b). This is one of the unique aspects of TAT rhodopsin. No photochromism at 77 K is disadvantageous for structural analysis such as low-temperature FTIR spectroscopy. Since there was no reversion after the illumination of the K intermediate in WT, we raised the temperature after obtaining a difference spectrum to complete the photocycle, and repeated the 10–13 recordings, as before [21].

Discussion

There are two rhodopsins, animal and microbial. In the case of animal rhodopsin, UV-absorbing pigments are known, in which the retinal Schiff base is deprotonated [16–18]. In contrast, all microbial rhodopsins possess a protonated retinal Schiff base. The M intermediate of archaeal sensory rhodopsin I (SRI_{373}), which contains an unprotonated Schiff base, is responsible for negative phototaxis [30], but this is the case for the intermediate. In such a situation, a newly found TAT rhodopsin contains a protonated and unprotonated Schiff base under physiological conditions because the pKa of the Schiff base coincides with the pH of the ocean (~8.0) [21]. The low pKa of the Schiff base is unique for TAT rhodopsin, allowing the two forms to exist in the native environment of the ocean (pH 8). Our recent study revealed that the photoreaction of the protonated form is complete within 10^{-5} sec, while that of the unprotonated form takes more than 10 sec [22]. Electrophysiology measurements showed that the extracellular pH affects the protonation equilibrium of the Schiff base. Based on these results, we proposed that TAT rhodopsin is a UV-dependent environmental pH sensor in marine bacteria [22]. When environmental pH is acidic, favoring the protonated Schiff base, absorbed visible light energy is quickly dissipated into heat without any functions. In contrast, when environmental pH becomes alkaline, absorption of UV/blue lights yields the formation of long-lived intermediates, possibly driving a signal transduction cascade in marine bacteria.

The present study reports that T82 is one of the determinants of unique properties of TAT rhodopsin. The pKa of the Schiff base (~8.0) increases significantly (pKa >10.5) with the T-to-D mutation (Fig. 3), indicating that T82 is responsible for the unusually low pKa of the Schiff base in TAT rhodopsin. In T82D, pH-dependent absorption changes were observed in the visible region (Fig. 3b), suggesting that the pKa of the Schiff base counterion is 8.1. Photoexcitation of T82D TAT rhodopsin yields a long photocycle (>10 sec) by forming M intermediates (Fig. 5b), which also support T82 being the determinant of the unusually fast photoreaction. No photoreaction of T82D at pH 6.0 indicates that two negative charges are necessary for the long photocycle (Fig. 5a). Although we did not analyse the chromophore configuration by HPLC in the present study, the all-trans form is probably responsible for the photocycle of T82D as well as WT [21].

Figure 7 summarizes the photoreactions after the absorption of visible light in WT (a), T82D at low pH (pH <8) (b), and T82D at high pH (pH >8) (c). As reported previously, light converts TAT rhodopsin into the K intermediate by an all-*trans* to 13-*cis* isomerization, which reverts to the original state without completing the photocycle (Fig. 7a). The situation is identical for T82D at low pH (pH <8) (Fig. 7b), as low-temperature UV-visible spectroscopy at 77 K monitored the formation of the K intermediate (Fig. 6b), but the photoreaction was complete within 10^{-5} sec (Fig. 5a). When D82 was negatively charged, the M intermediate appeared with a time constant of 57 μsec (Fig. 5b). We propose the photocycle scheme in Figure 7c, in which the M intermediate is formed from the K intermediate, followed by a branching reaction, where there is reversion to the original state with time-constants of 3.75 ms or 12.2 sec.

TAT rhodopsin has many unique aspects, which suggest a unique structure. However, this is not necessarily the case, and we suggest that TAT rhodopsin contains a similar structure to other microbial rhodopsins. In fact, a light-

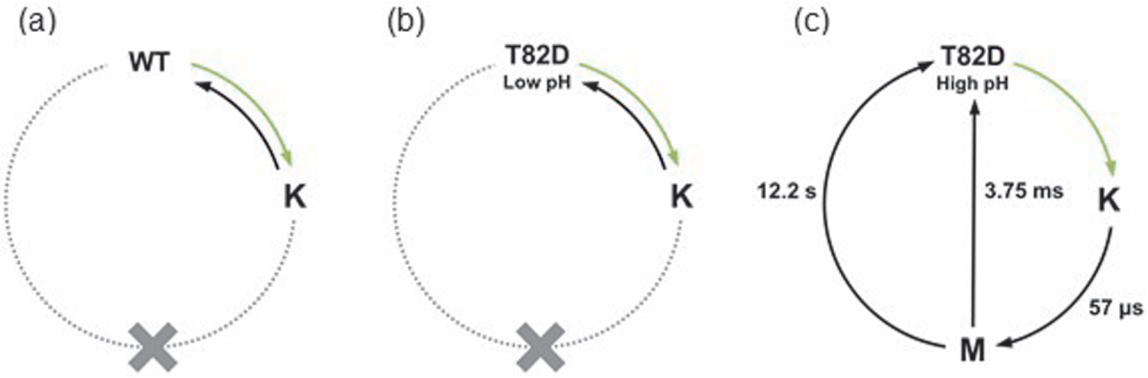

Figure 7 Photoreaction schema of the protonated form of WT (a), T82D at low pH (pH <8) (b), and T82D at high pH (pH >8) (c). Green arrows represent photoexcitation by green lights. In all cases, the primary intermediate is the red-shifted K intermediate, which is stabilized at 77 K. In the case of the protonated form of WT (a) and T82D at low pH (pH <8) (b), the K intermediate reverted to the original state within 10^{-5} sec. In the case of T82D at high pH (pH >8) (c), the M intermediate formed, which returned to the original state with time constants of 3.75 ms and 12.2 sec.

driven proton-pump BR contains a counterion complex of D85 and D212 (Fig. 1a), and the Schiff base pKa is very high (pKa >10). On the other hand, Brown *et al.* reported the Schiff base pKa of D85T BR to be 8.0 [31], which is very close to that of WT TAT rhodopsin. Halorhodopsin (HR) is a light-driven chloride pump, whose sequence motifs in the C helix are TSA. Therefore, T82 of TAT rhodopsin is also conserved in HR. The Schiff base pKa of *pharaonis* HR (*p*HR) is 8.0 in 150 mM sulfate and 9.6 in 150 mM chloride [32]. As *p*HR binds chloride, but not sulfate near the Schiff base, high pKa (9.6) is reasonable in *p*HR. On the other hand, the pKa value (8.0) in the absence of chloride is very close to that of WT TAT rhodopsin. Thus, TAT rhodopsin's structure around the Schiff base is presumably similar to those of other microbial rhodopsins, while TAT rhodopsin utilizes the unprotonated Schiff base for function.

Conclusion

The present study revealed that T82 is one of the determinants of the unique molecular properties of TAT rhodopsin since we observed an increased pKa of the Schiff base and a long photocycle for T82D. In T82D, the photocycle strongly depends upon the protonation state of D82. When D82 is neutral, transient absorption was completely silent at µs and slower timescales, which is identical to WT TAT rhodopsin, but this was never observed for known microbial rhodopsins. When D82 is negatively charged, the photocycle is very long. WT TAT rhodopsin switches to two distinct photoreactions that are dependent upon the protonation state of the Schiff base. Similarly, T82D TAT rhodopsin switches to two distinct photoreactions that are dependent upon the protonation state of D82. A further study will reveal the detailed molecular mechanism of the unique molecular properties of TAT rhodopsin. In particular, light-induced FTIR spectroscopy of TAT rhodopsin is our future focus.

Acknowledgements

This work was financially supported by grants from the Japanese Ministry of Education, Culture, Sports, Science and Technology to K.K. (18K14662) and H.K. (18H03986, 19H04959), and from Japan Science and Technology Agency (JST), PRESTO to K.K. (JPMJPR19G4) and CREST to H.K. (JPMJCR1753).

Conflicts of Interest

All authors declare that they have no conflicts of interest.

Author Contributions

H. K. directed the research and wrote the manuscript. T. T. prepared samples and performed all experiments with the help of K. K. T. T. and K. K. analyzed the data. All authors discussed and commented on the manuscript.

References

[1] Ernst, O. P., Lodowski, D. T., Elstner, M., Hegemann, P., Brown, L. S. & Kandori, H. Microbial and animal rhodopsins: Structures, functions, and molecular mechanisms. *Chem. Rev.* **114**, 126–163 (2014). DOI: 10.1021/cr4003769

[2] Shichida, Y. & Matsuyama, T. Evolution of opsins and photo-transduction. *Philos. Trans. R. Soc. Lond. B Biol. Sci.* **364**, 2881–2895 (2009). DOI: 10.1098/rstb.2009.0051

[3] Hofmann, K. P., Scheerer, P., Hildebrand, P. W., Choe, H-W., Park, J. H., Heck, M., *et al.* A G protein-coupled receptor at work: the rhodopsin model. *Trends Biochem. Sci.* **34**, 540–552 (2009). DOI: 10.1016/j.tibs.2009.07.005

[4] Palczewski, K. Chemistry and biology of vision. *J. Biol. Chem.* **287**, 1612–1619 (2012). DOI: 10.1074/jbc.R111.301150
[5] Haupts, U., Tittor, J. & Oesterhelt, D. Closing in on bacteriorhodopsin: progress in understanding the molecule. *Annu. Rev. Biophys. Biomol. Struct.* **28**, 367–399 (1999). DOI: 10.1146/annurev.biophys.28.1.367
[6] Lanyi, J. K. Bacteriorhodopsin. *Annu. Rev. Physiol.* **66**, 665–688 (2004). DOI: 10.1146/annurev.physiol.66.032102.150049
[7] Grote, M., Engelhard, M. & Hegemann, P. Of ion pumps, sensors and channels—perspectives on microbial rhodopsins between science and history. *Biochim. Biophys. Acta* **1837**, 533–545 (2014). DOI: 10.1016/j.bbabio.2013.08.006
[8] Brown, L. S. Eubacterial rhodopsins—Unique photosensors and diverse ion pumps. *Biochim. Biophys. Acta* **1837**, 553–561 (2014). DOI: 10.1016/j.bbabio.2013.05.006
[9] Inoue, K., Kato, Y. & Kandori, H. Light-driven ion-translocating rhodopsins in marine bacteria. *Trends Microbiol.* **23**, 91–98 (2015). DOI: 10.1016/j.tim.2014.10.009
[10] Govorunova, E. G., Sineshchekov, O. A., Li, H. & Spudich, J. L. Microbial rhodopsins: Diversity, mechanisms, and optogenetic applications. *Annu. Rev. Biochem.* **86**, 845–872 (2017). DOI: 10.1146/annurev-biochem-101910-144233
[11] Boyden, E. S., Zhang, F., Bamberg, E., Nagel, G. & Deisseroth, K. Millisecond-timescale, genetically targeted optical control of neural activity. *Nat. Neurosci.* **8**, 1263–1268 (2005). DOI: 10.1038/nn1525
[12] Deisseroth, K. Optogenetics. *Nat. Methods* **8**, 26–29 (2011). DOI: 10.1038/nmeth.f.324
[13] Hegemann, P. & Möglich, A. Channelrhodopsin engineering and exploration of new optogenetic tools. *Nat. Methods* **8**, 39–42 (2011). DOI: 10.1038/nmeth.f.327
[14] Pushkarev, A., Inoue, K., Larom, S., Flores-Uribe, J., Singn, M., Konno, M., *et al.* A distinct abundant group of microbial rhodopsins discovered using functional metagenomics. *Nature* **558**, 595–599 (2018). DOI: 10.1038/s41586-018-0225-9
[15] Singh, M., Katayama, K., Beja, O. & Kandori, H. Anion binding to mutants of the Schiff base counterion in heliorhodopsin 48C12. *Phys. Chem. Chem. Phys.* **21**, 23663–23671 (2019). DOI: 10.1039/c9cp04102h
[16] Shi, Y., Radlwimmer, F. B. & Yokoyama, S. Molecular genetics and the evolution of ultraviolet vision in vertebrates. *Proc. Natl. Acad. Sci. USA* **98**, 11731–11736 (2001). DOI: 10.1073/pnas.201257398
[17] Koyanagi, M., Kawano, E., Kinugawa, Y., Oishi, T., Shichida, Y., Tamotsu, S., *et al.* Bistable UV pigment in the lamprey pineal. *Proc. Natl. Acad. Sci. USA* **101**, 6687–6691 (2004). DOI: 10.1073/pnas.0400819101
[18] Yamashita, T., Ohuchi, H., Tomonari, S., Ikeda, K., Sakai, K. & Shichida, Y. Opn5 is a UV-sensitive bistable pigment that couples with Gi subtype of G protein. *Proc. Natl. Acad. Sci. USA* **107**, 22084–22089 (2010). DOI: 10.1073/pnas.1012498107
[19] Luck, M., Mathes, T., Bruun, S., Fudim, R., Hagedorn, R., Nguyen, T. M. T., *et al.* A photochromic histidine kinase rhodopsin (HKR1) that is bimodally switched by ultraviolet and blue light. *J. Biol. Chem.* **287**, 40083–40090 (2012). DOI: 10.1074/jbc.M112.401604
[20] Hontani, Y., Broser, M., Luck, M., Weißenborn, J., Kloz, M., Hegemann, P., *et al.* Dual photoisomerization on distinct potential energy surfaces in a UV absorbing rhodopsin. *J. Am. Chem. Soc.* **142**, 11464–11473 (2020). DOI: 10.1021/jacs.0c03229
[21] Kataoka, C., Inoue, K., Katayama, K., Béjà, O. & Kandori, H. Unique photochemistry observed in a new microbial rhodopsin. *J. Phys. Chem. Lett.* **10**, 5117–5121 (2019). DOI: 10.1021/acs.jpclett.9b01957
[22] Kataoka, C., Sugimoto, T., Shigemura, S., Katayama, K., Tsunoda, S. P., Inoue, K., *et al.* TAT rhodopsin is an ultraviolet-dependent environmental pH sensor. *Biochemistry* **60**, 899–907 (2021). DOI: 10.1021/acs.biochem.0c00951
[23] Inoue, K., Ono, H., Abe-Yoshizumi, R., Yoshizawa, S., Ito, H., Kogure, K., *et al.* A light-driven sodium ion pump in marine bacteria. *Nat. Commun.* **4**, 1678–1687 (2013). DOI: 10.1038/ncomms2689
[24] Inoue, K., Ito, S., Kato, Y., Nomura, Y., Shibata, M., Uchihashi, T., *et al.* A natural light-driven inward proton pump. *Nat. Commun.* **7**, 13415–13424 (2016). DOI: 10.1038/ncomms13415
[25] Bergo, V. B., Sineshchekov, O. A., Kralj, J. M., Partha, R., Spudich, E. N., Rothschild, K. J., *et al.* His-75 in proteorhodopsin, a novel component in light-driven proton translocation by primary pumps. *J. Biol. Chem.* **284**, 2836–2843 (2009). DOI: 10.1074/jbc.M803792200
[26] Hempelmann, F., Holper, S., Verhoefen, M. K., Woerner, A. C., Kohler, T., Fiedler, S. A., *et al.* His75-Asp97 cluster in green proteorhodopsin. *J. Am. Chem. Soc.* **133**, 4645–4654 (2011). DOI: 10.1021/ja111116a
[27] Balashov, S. P., Petrovskaya, L. E., Lukashev, E. P., Imasheva, E. S., Dioumaev, A. K., Wang, J. M., *et al.* Aspartate-histidine interaction in the retinal Schiff base counterion of the light-driven proton pump of *Exiguobacterium sibiricum*. *Biochemistry* **51**, 5748–5762 (2012). DOI: 10.1021/bi300409m
[28] Gushchin, I., Chervakov, P., Kuzmichev, P., Popov, A. N., Round, E., Borshchevskiy, V., *et al.* Structural insights into the proton pumping by unusual proteorhodopsin from nonmarine bacteria. *Proc. Natl. Acad. Sci. USA* **110**, 12631–12636 (2013). DOI: 10.1073/pnas.1221629110
[29] Kandori, H. Structure/function study of photoreceptive proteins by FTIR spectroscopy. *Bull. Chem. Soc. Jpn.* **93**, 904–926 (2020). DOI: 10.1246/bcsj.20200109
[30] Spudich, J. L. & Bogomolni, R. A. Mechanism of colour discrimination by a bacterial sensory rhodopsin. *Nature* **312**, 509–513 (1984). DOI: 10.1038/312509a0
[31] Brown, L. S., Bonet, L., Needleman, R. & Lanyi, J. K. Estimated acid dissociation constants of the Schiff base, Asp-85, and Arg-82 during the bacteriorhodopsin photocycle. *Biophys. J.* **65**, 124–130 (1993). DOI: 10.1016/S0006-3495(93)81064-6
[32] Scharf, B. & Engelhard, M. Blue halorhodopsin from *Natronobacterium pharaonis*: wavelength regulation by anions. *Biochemistry* **33**, 6387–6393 (1994). DOI: 10.1021/bi00187a002

(*Edited by Yoshinori Shichida*)